

Contribution from the Chemistry Department,
University of Chicago, Chicago, Illinois 60637

Structural Correlations in Small Molecules: A Simple Molecular Orbital Treatment of *sp* Mixing

JEREMY K. BURDETT

Received November 9, 1978

Simple molecular orbital theory in the form of the angular-overlap model is used to assess the changes in bond stabilization energy as a result of *sp* mixing as the angular geometry of a molecule changes. The results reproduce well qualitative aspects of the observed bond shortenings and elongations (described by Bürgi, Dunitz, Murray-Rust, and colleagues) in C_{3v} , C_{2v} , and D_{2d} MX_4 molecules compared to T_d , C_{2v} MX_3 molecules compared to D_{3h} , and C_{3v} MX_5 molecules compared to D_{3h} . A study of the Berry process highlights differences between five-coordinate transition-metal and main-group systems. A hierarchy of perturbations causing structural change is described.

Introduction

The principle of structural correlation has been used with great success by Bürgi, Dunitz, Murray-Rust, and co-workers¹⁻⁷ to map out the minimum-energy pathways in associative (e.g., S_N2 at¹ tetrahedral Cd^{II}) and dissociative (e.g., S_N1 at² tetrahedral MX_4 and MX_3Y ; $M = Al, Sn, P, S; X, Y = Hal, O$) reactions. Results³ for the S_N1 case are shown in Figure 1 where, irrespective of the nature of $M, X,$ and $Y,$ the points representing the bond length changes as a function of geometry are superimposable. This insensitivity of the observation to the nature of the central atom and ligands is most striking. Perhaps even more interesting is that the two curves are well fitted by eq 1 and 2. These are of the same

$$\Delta r_a = -0.5 \log (9 \cos^2 \theta) \quad (1)$$

$$\Delta r_b = -0.5 \log (\frac{4}{3} - 3 \cos^2 \theta) \quad (2)$$

form as the Pauling bond length/bond number relationship⁸ $\Delta r_i = c_i \log n_i$ where n_i is the bond order and c_i a constant. Satisfyingly, the total bond order around the central atom is $\sum_{i=1}^4 n_i = 4$ for all values of θ from eq 1 and 2. Thus the total "valency" at the M atom remains constant on distortion. A bond length dependence on the secant of the O-T-O angle has been shown^{3b} to hold for $T = Si, Ge, As, S,$ and Se from an assessment of both observed structural data and bond overlap populations from MO calculations on silicates, germanates, etc.

The changes in bond length in this system may also be understood in terms of valence-bond arguments concerning the strength of the various sp^n hybrids as the geometry is changed. Thus at the tetrahedral geometry ($\theta = 71^\circ$), all four ligands are attached by sp^3 hybrids. As θ increases, the basal ligands are bound by hybrids containing less p character (sp^2 at $\theta = 90^\circ$) and are therefore stronger. The axial ligand at this stage is bound by a pure p orbital, and this MX bond is correspondingly weakened. For other geometry changes, especially those involving five-coordinate systems or transition-metal complexes, such qualitative arguments are not very good. In this paper we view these structural changes with simple molecular orbital ideas.

Molecular Orbital Description of Molecular Deformations

The basis of our molecular orbital approach will be the angular-overlap model⁹ which we have described extensively elsewhere.¹⁰ While used almost exclusively in the past for the study of the electronic and magnetic properties of transition-metal complexes, in our hands it has been successfully used to view structural^{11,12} and kinetic¹³ aspects of both main-group¹⁴ and transition-metal-containing systems. Briefly, the interaction energy ϵ (equal to the stabilization energy of the bonding orbital and perhaps approximately equal to the destabilization energy of the antibonding orbital) of two single

orbitals or symmetry-adapted linear combinations φ_i and φ_j is given by a power series in the overlap integral S_{ij} between them (eq 3); β and γ are constants. In most instances we have

$$\epsilon = \beta S_{ij}^2 - \gamma S_{ij}^4 + \dots \quad (3)$$

included the lead term only and written eq 4, where β is a

$$\epsilon = \beta S_{ij}^2 \quad (4)$$

constant inversely proportional to the energy separation between the two initial orbitals φ_i and φ_j . Thus the closer two orbitals are in energy and the larger their overlap, the larger their mutual interaction. The beauty of the approach is that S_{ij} may be written as a simple function of the angular disposition of orbital i relative to j (eq 5) where Θ and Φ are polar

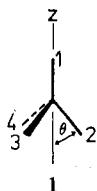
$$S_{ij} = S_\lambda(f(\Theta, \Phi)) \quad (5)$$

coordinates. S_λ is a constant for a given $M, X,$ and MX distance ($\lambda = \sigma, \pi$), but $f(\Theta, \Phi)$ is the same for all orbitals of a given type ($s, p, d,$ etc.) irrespective of the nature of $M, X,$ or the principal quantum number of the orbital.

Our strategy will be to calculate, with this model, the total stabilization energy of a given $MX_{3,4,5}$ molecule as a function of geometry (e.g., θ of Figure 1), keeping all bond lengths equal (S_λ constant). We will then see if there is any correlation between the observed bond lengths and the calculated stabilization energies associated with each symmetry-unrelated bond in the molecule.

The energy diagram for the $M + X_{3,4,5}$ system consists of an ns orbital at low energy on the M atom (M_s) and an np orbital (M_p) at a higher energy. Intermediate in energy for main-group systems are the ligand σ orbitals. We shall consider metal-ligand σ interactions only since these may be expected to be dominant. We will switch on the $M-X\sigma$ interaction in two parts. First we turn on the $M_s-X\sigma$ interaction, and second we view the M_p interaction with the resulting orbitals. We have included such sp mixing in our deliberations before,¹⁴ but here it is introduced in quantitative fashion. We will find that the $M_s-X\sigma$ nonbonding orbital plays a vital role in controlling the structural dynamics of the system. Interestingly, a study by Shustorovich¹⁵ which addresses itself to the problem of how the nature of one ligand in an MX_n complex affects the bond properties of another finds a crucial role for this particular orbital. Shustorovich's method, also one based on perturbation theory, is interested in bond length changes induced by changing the nature of one of the ligands. Here we are interested in similar structural changes induced by angular adjustments to the symmetric geometry.

C_{3v} Distortion of the Tetrahedron. We will describe this situation in detail in order to show how our simple approach works in practice. There is one angular degree of freedom (**1**) associated with this distortion coordinate. Figure 2a shows the interaction between the M_s orbital (a_1) and the ligand σ



a_1 combinations. In the C_{3v} geometry there are two ligand σ a_1 combinations, one of which in the absence of ligand–ligand overlap contains no Ms character and is M–X nonbonding. In the tetrahedron (T_d) it merges with the e pair of ligand σ orbitals to form the t_2 trio. The result of the Ms–X σ interaction is three a_1 orbitals (j, k, l). We may immediately write down the form of the wave functions as in Figure 2a. The values of a , b , a' , and b' will not concern us. (They are set of course by the actual size of Ms–ligand σ interaction.) The most important feature is our ability to write down a wave function ψ_k for orbital $a_1(k)$ which is determined only by its being MX σ nonbonding and orthogonal to $a_1(j)$ and $a_1(l)$. The lowest four orbitals are doubly filled in these systems (e.g., $AlCl_4^-$), and from our interaction energy eq 4 and the substitution of eq 5, the total σ stabilization energy (which we write as $\Sigma(\sigma)$) is given by twice the stabilization energy of the $a_1(l)$ orbital and is simply $\Sigma(\sigma) = 8\beta_s S_s^2$ where the parameters β_s and S_s are those appropriate to Ms–X σ interaction. No angular dependence arises in this equation since Ms–X σ overlap integrals are isotropic ($f(\theta, \Phi) = 1$). The bond stabilization energy from this source is then for each bond $\Sigma(\sigma) = 2\beta_s S_s^2$ ($i = 1-4$).

When the Mp interactions are switched on (Figure 2b), there are three stabilizing interactions of occupied orbitals to consider, those with the ligand e symmetry σ orbitals and those with $a_1(k)$ and $a_1(l)$ orbitals. The energy separation Mp/ $a_1(l)$ is greater than the Ms/Mp energy separation in the free atom and will be larger than the Mp/ $a_1(k)$ energy separation. From the nature of the β constant in eq 4 (inversely dependent on energy separation) the interaction of Mp with $a_1(k)$ will be larger than that with $a_1(l)$. In addition, $a_1(k)$ is a pure ligand orbital and in general may be expected to have a larger overlap integral with Mp than with the $a_1(l)$ orbital (largely Ms in character). We shall therefore neglect the Mp– $a_1(l)$ interactions. In contrast to Ms–X σ interactions, the Mp–X σ interactions are angle dependent.¹⁶ Specifically if α is the angle the M–X vector makes with the z axis, the σ overlap integral with p_z is $S_p \cos \alpha$. The ligand σ combinations of species e involve the basal ligands only (see 1 for ligand labels).

$$\psi_e(1) = (1/\sqrt{2})(\varphi_4 - \varphi_3) \quad (6)$$

$$\psi_e(2) = (1/\sqrt{6})(2\varphi_2 - \varphi_3 - \varphi_4)$$

Evaluation of the overlap integrals of these functions with Mp leads to $\epsilon = \frac{3}{2}(\sin^2 \theta)\beta_p S_p^2$ for each component and a basal ligand stabilization energy (eq 7) for each ligand, where the

$$\Sigma_b(\sigma) = 2(\sin^2 \theta)\beta_p S_p^2 \quad (7)$$

parameters $\beta_p S_p^2$ are those appropriate for Mp–X σ interaction. The overlap integral between Mp and ψ_k is given simply by eq 8 where the geometry-independent term contains all the

$$S = (1/\sqrt{12})(3 + 3 \cos \theta)S_p \quad (8)$$

axial ligand contribution and the geometry-dependent term the overlap arising from the basal ligands. On squaring eq 8 for substitution into eq 4, axial/basal “cross terms” appear. We divide these equally between the two different bonds (axial and basal) in the molecule as we have done on previous occasions.^{14,17} This leads to contributions to the bond stabilization energies given by eq 9. Collection of all the stabilization energies together gives the result of eq 10. At the tetrahedral

$$\begin{aligned} \Sigma_a(\sigma) &= \frac{3}{2}(1 + \cos \theta)\beta_p S_p^2 \\ \Sigma_b(\sigma) &= \frac{1}{2}(\cos \theta)(1 + \cos \theta)\beta_p S_p^2 \end{aligned} \quad (9)$$

$$\begin{aligned} \text{total } \Sigma_a(\sigma) &= 2\beta_s S_s^2 + \frac{3}{2}(1 + \cos \theta)\beta_p S_p^2 \\ \text{total } \Sigma_b(\sigma) &= 2\beta_s S_s^2 + 2[1 - \frac{1}{4}(\cos \theta)(3 \cos \theta - 1)]\beta_p S_p^2 \end{aligned} \quad (10)$$

geometry, $\Sigma_a(\sigma) = \Sigma_b(\sigma) = 2(\beta_s S_s^2 + \beta_p S_p^2)$. The difference in stabilization energy between a distorted geometry and tetrahedral is simply given by eq 11. A plot of $-\Delta_{a,b}$ against

$$\begin{aligned} \Delta_a &= \frac{1}{2}(3 \cos \theta - 1)\beta_p S_p^2 \\ \Delta_b &= -\frac{1}{2}(\cos \theta)(3 \cos \theta - 1)\beta_p S_p^2 \end{aligned} \quad (11)$$

θ leads¹⁸ to a very similar diagram (Figure 3) to Figure 1 (i.e., increasing stabilization energy leads to shorter bond lengths). The only qualitative discrepancy is the performance of our curve for the basal ligands at $\theta = 90^\circ$ (the planar MX_3 geometry). The ratio (–3) of the two slopes of the curves at $\theta =$ the tetrahedral angle is a symmetry property of our molecular orbital model and, as it turns out, of the experimental data too.

An exactly equivalent description of the main features of the change in bond stabilization energy with θ is reached if the s–p mixing is applied in the opposite sense to the way we have treated it above; i.e., we view s-orbital interaction with a set of orbitals determined by Mp–X σ interaction. Again the key orbital is $a_1(k)$ which on a p-orbital-only model may be written as eq 12 where d measures the size of Mp–X σ

$$\psi_k = c[\varphi_1 - (\cos \theta)(\varphi_2 + \varphi_3 + \varphi_4) + d\varphi_p] \quad (12)$$

interaction, and c is a normalization factor. The Ms orbital is stabilized by a total interaction of $4\beta_s S_s^2$ as before. The overlap integral of ψ_k with Ms needed to evaluate the destabilization energy of this $a_1(k)$ orbital is $c(1 - 3 \cos \theta)S_s$. Division of the cross term between axial and basal linkages gives eq 13 where the normalization constant c contains some

$$\Sigma_a(\sigma) = 2(\beta_p S_p^2 + \beta_s S_s^2) + 2c^2(3 \cos \theta - 1)\beta_s S_s^2 \quad (13a)$$

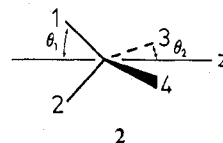
$$\Sigma_b(\sigma) = 2(\beta_p S_p^2 + \beta_s S_s^2) + 2c^2(3 \cos \theta - 1)(-\cos \theta)\beta_s S_s^2 \quad (13b)$$

function of the $\beta_p S_p^2$ expression via the term d in eq 12. While the units of the changes in $\Sigma(\sigma)$ in eq 14 are different ($c^2\beta_s S_s^2$)

$$\begin{aligned} \Delta_a &= 2c^2(3 \cos \theta - 1)\beta_s S_s^2 \\ \Delta_b &= -2c^2(\cos \theta)(3 \cos \theta - 1)\beta_s S_s^2 \end{aligned} \quad (14)$$

from those of eq 11 ($\beta_p S_p^2$), the angular variation in bond stabilization energy is identical. (A small difference does actually occur since $\cos^2 \theta$ occurs in the normalization procedure to establish the constant c .) In the rest of our discussion we shall, however, use the original order of interaction in looking at sp mixing, but remember that an analogous angular dependence is found if the reverse procedure is used. The fact that the associated (non- θ -containing) terms are different in the two approaches should warn us off trying to comment too seriously on the variation of the absolute size of the effect from one M/X system to another.

C_{2v} Distortion of the Tetrahedron. There are two angular degrees of freedom in this coordinate (2). Figure 4 shows



the orbital symmetries and form of the a_1 orbitals before Mp

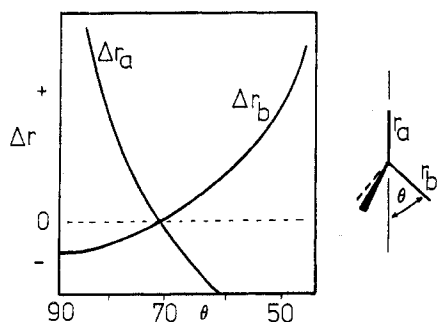


Figure 1. Observed structural correlations on C_{3v} distortion of four-coordinate, main-group molecules (adapted from ref 3).

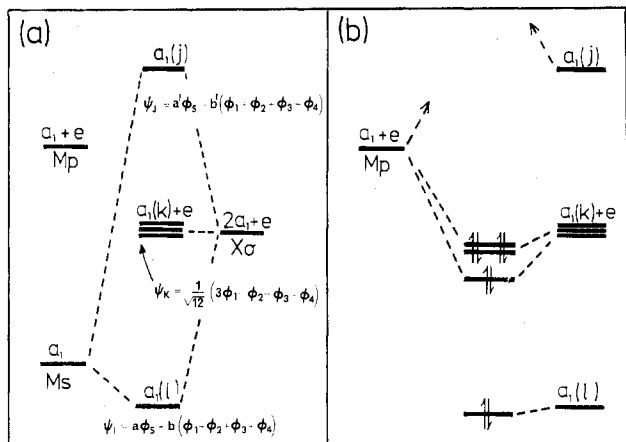


Figure 2. (a) Resulting molecular orbitals on switching on $M_s-X\sigma$ interactions in a C_{3v} MX_4 system. Three a_1 orbitals result: j, k, l. (b) Result of switching on $M_p-X\sigma$ interaction with the ligand σ e set and these a_1 orbitals. These diagrams are obtained by leaving all MX bond lengths the same and ignoring $X\cdots X$ interactions. This means that the effective symmetry of the X_4 fragment is S_4 (symmetric group of order four and isomorphic to T_d).

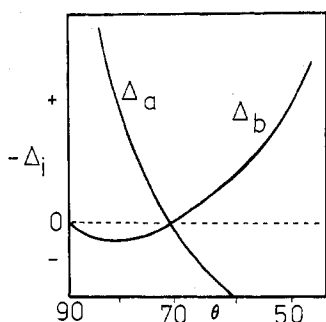


Figure 3. Plot of $-\Delta_i$ (units $\beta_p S_p^2$) against θ for axial (a) and basal (b) MX bonds. Compare this with the observed Δr against θ plots of Figure 1.

interaction for the C_{2v} geometry. Application of the method readily gives the pair of functions (eq 15) describing the energy

$$\begin{aligned} \Delta_{1,2} &= (\cos \theta_1)(\cos \theta_2 - \cos \theta_1)\beta_p S_p^2 \\ \Delta_{3,4} &= (\cos \theta_2)(\cos \theta_1 - \cos \theta_2)\beta_p S_p^2 \end{aligned} \quad (15)$$

differences from the tetrahedral structure. These show that the change in stabilization energy (and hence bond length) as a result of a change in angle should be of the opposite sign depending upon whether the angle is the included angle (θ_1 for r_1 and r_2) or the opposite angle (θ_2 for r_1 and r_2). This result is neatly borne out by the recent analysis of Baur's collection¹⁹ of 211 phosphate ion structures by Murray-Rust, Bürgi, and Dunitz.⁶ As θ_1 decreases ($\cos \theta_1$ increases) so the bond length r_1 increases, but as θ_2 decreases ($\cos \theta_2$ increases)

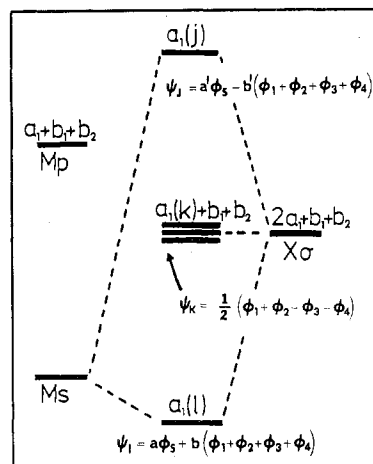


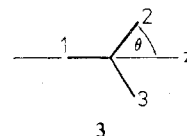
Figure 4. Resulting molecular orbitals on switching on $M_s-X\sigma$ interactions in a C_{2v} MX_4 system.

so the bond length r_1 decreases. Interestingly, for D_{2d} (and D_{4h} square planar) geometries, where $\theta_1 = \theta_2$, $\Delta_{1,2} = \Delta_{3,4} = 0$. In both these geometries, sp mixing is not allowed by symmetry (D_{2d} $s \rightarrow a_1$, $p \rightarrow b_2 + e$; D_{4h} $s \rightarrow a_{1g}$, $p \rightarrow e_u + a_{2u}$), and this particular bond weakening/strengthening process cannot occur. From Baur's collection of phosphate structures,¹⁹ only that of $LuPO_4$ had a D_{2d} phosphate ion. In agreement with our molecular orbital approach, the bond lengths in the ion are found to be very close to those found in regular tetrahedral phosphates.

Our method then gives a correct bond length dependence on angular geometry. It is difficult to use this simple method to decide which of the three distortions we have analyzed (C_{3v} , D_{2d} , C_{2v}) is of lowest energy, but rather, given a distortion, we may predict how the bond lengths in the molecule change.

As is clear from a survey of the literature and will be mentioned later several times in this paper, transition-metal complexes with incomplete d shells ($<d^{10}$) possess structural features which are often very different from their main-group analogues. Thus for a $T_d \rightarrow D_{2d} \rightarrow D_{4h}$ distortion of (for example) a d^9 species where d-orbital forces are large (see later), we expect to see bond length changes arising via differential metal d-ligand σ interactions between the various geometries. At the tetrahedral geometry, the d-orbital stabilization energy per bond is $0.33\beta_\sigma S_\sigma^2$ (the units are the parameters we use to describe these d-orbital interactions^{10,11}), and at the square planar it is $0.75\beta_\sigma S_\sigma^2$. On the d-orbital-only model the $CuCl$ bond should therefore shorten as d^9 $CuCl_4^{2-}$ species move to planar. In fact there is not a well-defined bond length change in the structures available. (The scatter of points has been interpreted⁴ as indicative of the opposite change in bond length.)

C_{2v} Distortion of a Trigonal Plane. The results of the $D_{3h} \rightarrow C_{2v}$ (T shape) distortion (3) of a three-coordinate geometry



are very similar to those for the $T_d \rightarrow C_{3v}$ distortion of the four-coordinate one. We readily derive the functions (eq 16)

$$\begin{aligned} \Delta_1 &= \frac{4}{3}(\cos \theta - \frac{1}{2})\beta_p S_p^2 \\ \Delta_{2,3} &= -\frac{4}{3}(\cos \theta)(\cos \theta - \frac{1}{2})\beta_p S_p^2 \end{aligned} \quad (16)$$

which are closely related in form to the functions of eq 11. Here there is a symmetry-determined ratio of the slopes of the two curves of -2 at the trigonal-planar geometry. Distortions of three-coordinate molecules of this type do indeed follow plots

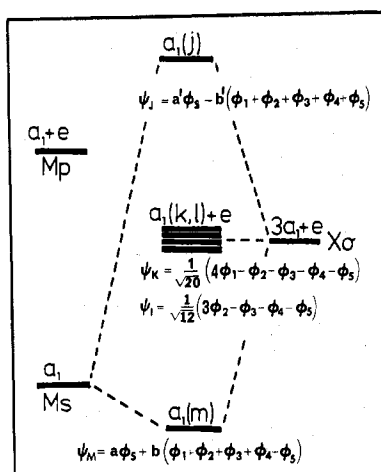
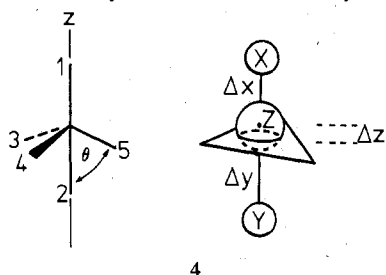


Figure 5. Resulting molecular orbitals on switching on Ms-X σ interactions in a C_{3v} MX_5 system. Here the effective symmetry of the X_5 unit is S_5 , the symmetric group of order five, since all MX bond lengths are equal and X...X interactions are ignored.

which are similar to those of the C_{3v} distortion of the tetrahedron.⁷ Examples include nitrate ions where the distortions are relatively small to some $M^I\text{HalL}_2$ species²⁰ ($M = \text{Cu, Ag, Au}$) and Hg^{II} systems²¹ (all d^{10}) where often the LML angle approaches 180° and the M-Hal distance is long.²² The low-spin, d^8 , T-shaped molecule $\text{Rh}(\text{PPh}_3)_3^+$, however, does not²³ have a long unique M-P bond. The shape of this molecule is precisely that expected^{11,24,25} for a $1s\ d^8$ system where the geometry is controlled by d-orbital forces, and the sp mixing scheme, described here, is perhaps of secondary importance.

C_{3v} Distortion of a Trigonal Bipyramid. An exactly analogous method may be used to view this system. 4 defines



the geometrical parameters of the system and relates them to the Δr used in Bürgi's analysis.¹ Since $r_{3,4,5}$ are found experimentally to hardly change during the distortion ($\theta = 71-90^\circ$), then $\Delta z = r_3 \cos \theta = 2.52 \cos \theta$. Figure 5 shows the Ms-X σ interaction part of the diagram, and as before we may immediately write down the wave functions for the two a_1 orbitals labeled k and l which we will need later. Ms-X σ interaction gives an s-orbital stabilization energy of $\sum_i(\sigma) = 2\beta_s S_s^2$ as before. In contrast to the four- and three-coordinate cases, we have two nonbonding a_1 ligand σ orbitals. Evaluation of the relevant Mp-X σ overlap integrals allows ready calculation of the $\sum_i(\sigma)$ from this source, and a little rearrangement gives the expressions (17) for the difference in

$$\begin{aligned} \Delta_1 &= \frac{1}{5}(\cos \theta)\beta_p S_p^2 & \Delta_2 &= -\frac{1}{5}(\cos \theta)\beta_p S_p^2 \\ \Delta_{3,4,5} &= -\frac{1}{5}(\cos^2 \theta)\beta_p S_p^2 \end{aligned} \quad (17)$$

stabilization energy between trigonal-bipyramidal (D_{3h} , $\theta = 90^\circ$) and distorted (C_{3v} , $\theta \neq 90^\circ$) structures.

These equations qualitatively mirror the observed¹ behavior. The changes in the two axial MX distances found experimentally are found to fit the same function but for a sign change which is indicated also in eq 17. In addition, there is no change within experimental error in the bond lengths $r_{3,4,5}$

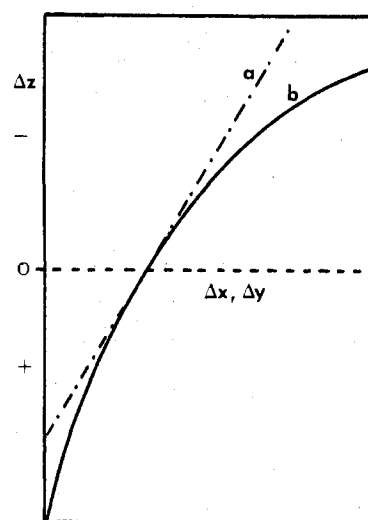


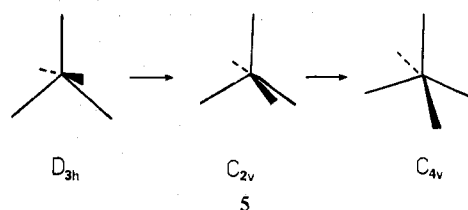
Figure 6. Observed structural correlation and calculated $-\Delta_i$ for the C_{3v} distortion of an MX_5 system (S_N2 process at tetrahedral MX_4): (a) calculated variation of $-\Delta_i$ as a function of θ and Δz of 4; (b) least-squares-refined curve obtained by Bürgi¹ from the experimental data for the bond length changes Δx and Δy .

as the molecule is distorted. This is well described by a Δ_3 which is less than one-fifth of $\Delta_{1,2}$ for a change in θ of 10° . Figure 6 shows a plot of $-\Delta_{1,2}$ against the observed data and Bürgi's least-squares-refined curve for the Cd^{II} system.

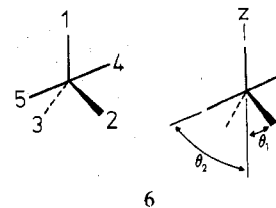
Bürgi was tempted to suggest by his analysis of the data that the axial ligands were bound mainly by ionic bonds.¹ Our molecular orbital approach to the problem is of course a covalent one. It does also involve the high-energy 5p orbital on Cd^{II} that was suggested not to be of importance in determining the structural changes.²⁶

The Berry Process in Five-Coordinate Molecules

The geometries of a large number of five-coordinate molecules are described by the Berry scheme (5). The



molecule has C_{2v} symmetry at least (6). For $\theta_1 = 90^\circ$ and



$\theta_2 = 60^\circ$, a trigonal bipyramid (TBP) results and for $\theta_1 = \theta_2$ a square pyramid (SPY). A spectrum of geometries linking one extreme to another is pictorially displayed by Muetterties and Guggenburger.²⁷ Application of our method gives eq 18 describing the bond stabilization energies as a function of geometry.

$$\sum_1(\sigma) = \frac{1}{5}[2 + \cos \theta_1 + \cos \theta_2]\beta_p S_p^2 + 2\beta_s S_s^2 \quad (18a)$$

$$\sum_{2,3}(\sigma) = [2 + \frac{2}{5}(\cos \theta_1)(1 - \cos \theta_1 - \cos \theta_2)]\beta_p S_p^2 + 2\beta_s S_s^2 \quad (18b)$$

$$\sum_{3,4}(\sigma) = [2 + \frac{2}{5}(\cos \theta_2)(1 - \cos \theta_1 - \cos \theta_2)]\beta_p S_p^2 + 2\beta_s S_s^2 \quad (18c)$$

Table I. Bond Stabilization Energies in Five-Coordinate Geometries for Main-Group and Transition-Metal Systems

		bond number (6)		
		1	2,3	4,5
present ^a scheme	SPY	$8/5$	2	2
(units $\beta_p S_p^2$)	TBP	2	2	2
d-orbital-only model, ^b	SPY	0	$3/4j$	$3/4j$
(units $\beta_\sigma S_\sigma^2$)	TBP	$1/4j$	j	$1/4j$

^a Bond stabilization energy is $2\beta_p S_p^2$ plus the entry in the table.
^b $j = 2$ for low-spin d^8 ; $j = 1$ for d^9 (see ref 12).

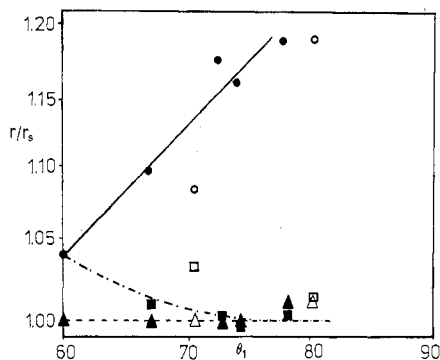
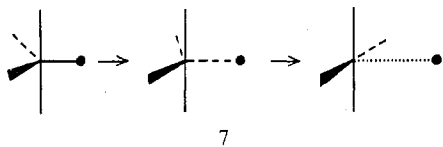


Figure 7. Structural correlation in MX_5 molecules—loss of an axial ligand from a trigonal bipyramid (7). Observed results for $CuCl_5^{3-}$ (adapted from ref 7) and $Ni(CN)_5^{3-}$ systems (from ref 32). Circles represent r_1 (see 6), squares the average value of r_2 and r_3 , and triangles the average value of r_4 and r_5 . Solid symbols are for $CuCl_5^{3-}$. Open symbols are for $Ni(CN)_5^{3-}$. r/r_s is the ratio of a given bond length to the average value found for r_4 and r_5 in the trigonal bipyramid or geometry closest to it.

Table I gives the values of $\sum_i(\sigma)$ for the three symmetry-unrelated sets of bonds at TBP and SPY geometries. We also include values using a d-orbital-only model for the $1s d^8$ and d^9 transition-metal complex from our previous discussions.¹² There has been no detailed structural correlation discussion for the main-group systems, and so we concentrate our effort on these transition-metal examples. For these species, the d-orbital-only model fits the observed structural trends very well (Figures 7 and 8) and emphasizes the superiority of d orbital compared to s,p orbital forces for these particular configurations. We have commented on the apparent weakness of the s,p forces in this system before.¹² Both $1s d^8$ ($Ni(CN)_5^{3-}$) and d^9 ($CuCl_5^{3-}$) are plotted on the same diagram in Figure 7. This equatorial ligand loss from the TBP (7) is one we have viewed before.¹³ It is the process suggested



to occur in substitution reactions of square-planar (especially $1s d^8$) systems.

From the structural correlation data,⁷ the S_N2 pathway via loss of an axial ligand from the TBP for these chlorocuprates was not a favored dissociation pathway (contrast with the Cd^{II} results above). If the d-orbital forces do determine the reaction pathway, then it is noteworthy that the resultant tetrahedral structure in the present case would be Jahn-Teller unstable and represent a local energy maximum. A scatter plot of the Berry pathway (in terms of $\theta_1\theta_2$ values) shows⁵ that the axial-basal angle of the SPY is smaller for the transition-metal d^8 and d^9 examples than for the main-group systems. This is probably a natural consequence of the fact that the axial

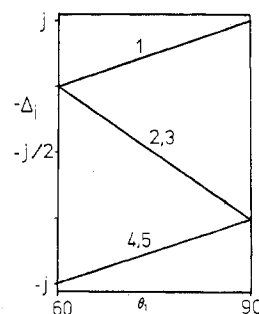


Figure 8. Calculated variation in $-\Delta_i$ (units of $\beta_\sigma S_\sigma^2$) with geometry for the d-orbital-only model for the Berry process of 6 and 7. We have only calculated the end points and linearly interpolated the geometries between ($j = 1$ (d^9), 2 ($1s d^8$)). The numbers represent the contributions to each of the bonds labeled in 6. (A better comparison with the data of Figure 7 is found if $1/\Delta_i$ is plotted.)

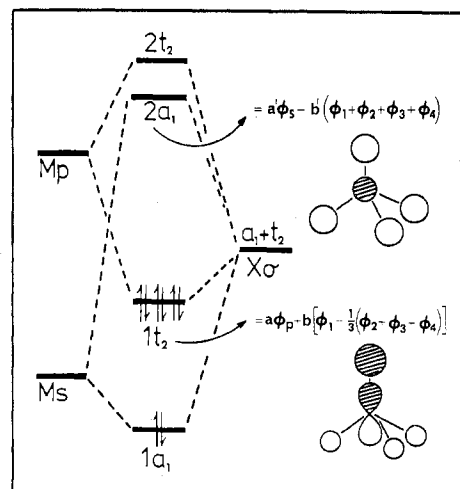


Figure 9. Molecular orbital diagram for an MX_4 system showing explicitly the form of the $2a_1$ and one component of the $1t_2$ orbitals which mix together on a reduction of symmetry to C_{3v} .

ligand is strongly bound and takes an active part in the stereochemistry of the main-group systems. In the transition-metal examples it is only rather weakly attached (especially in the $CuCl_5^{3-}$ system where, unlike¹² the case of the $Ni(CN)_5^{3-}$ ion, there is no π stabilization energy) to a basically square-planar structure.

An Alternative Approach

Another method which sheds light on the distortions in these systems is the application of simple perturbation theory to the molecular orbital diagram of the symmetric geometry. Figure 9 shows the molecular orbital scheme for the tetrahedral MX_4 species with the form of the $1t_2$ and $2a_1$ orbitals shown explicitly. On applying a C_{3v} perturbation by changing the angle θ , the $1t_2$ orbital splits into an e and a_1 . The a_1 component may now mix with all the other a_1 orbitals in the molecule, the size of the interaction being governed by the rules of perturbation theory.²⁸ The form of this new a_1 orbital is approximately given by eq 19 where "tet" refers to the tet-

$$\psi(a_1) = \psi(1t_2)_{tet} + (V/\hbar\omega)\psi(2a_1)_{tet} \quad (19)$$

rahedral geometry, V is a measure of the size of the perturbation, and $\hbar\omega$ is the $1t_2/2a_1$ energy separation. This equation has ignored the mixing expected between $1t_2$ and $1a_1$.²⁹ In the $2a_1$ orbital we expect $b' > a'$ (Figure 9), and so the dominant change in overlap population will come from the product of ligand combination $b'(\phi_1 + \phi_2 + \phi_3 + \phi_4)$ from $2a_1$ with the central atom a_ϕ function from $1t_2$ (eq 20). Since the overlap integral of a basal ligand σ orbital with p_z is $-1/3$ of that for an axial ligand at the tetrahedral geometry, the

$$\begin{aligned} \text{change in } M-X_a \text{ population} &\propto \int \varphi_1 \varphi_p \, d\tau \\ \text{change in } M-X_b \text{ population} &\propto \int \varphi_{2,3,4} \varphi_p \, d\tau \end{aligned} \quad (20)$$

change in bond-overlap population is 3 times larger for the axial MX linkage than for the basal one, and of the opposite sign. The effect increases with increasing $Mp-X\sigma$ overlap integral. (On perturbation, the lower a_1 component (from $1t_2$) will always be lowered in energy. This therefore controls the phase with which $2a_1$ and $1t_2$ mix together when θ is increased or decreased, i.e., whether the axial bond-overlap population decreases and the basal increases or vice versa.) Similar arguments may be used to view distortions in the other systems we have analyzed above. The result is quite analogous to that obtained by use of related perturbation formalism of the second-order Jahn-Teller treatment.

In addition to predicting a larger effect on the bond-overlap populations as $Mp-X\sigma$ interaction is increased, the mixing of the $1t_2$ and $2a_1$ orbitals will be smaller the larger the $1t_2/2a_1$ gap ($\hbar\omega$ above). This will be set by the size of the $Ms-X\sigma$ interactions. Thus as before,¹⁸ the observed bond length changes are a result of competition by Ms and Mp orbitals for maximum bonding to the ligand σ orbitals.

Discussion

To begin, we point out that there is a strong symmetry element to our approach and apparently of the data too. For example, the relative slopes (-3) of the two curves of Figure 3 at the tetrahedral geometry is symmetry determined. What we have been able to match however is the observed weakening and strengthening of particular bonds in the molecule as a function of angle with a chemically interesting approach. Not all simple approaches (see below) give the right answer!

Our approach is based on a method where the geometry-determining part (the $f(\theta, \Phi)$ of eq 5) is independent of the nature of M , X , or Y (i.e., the angular shape of a p orbital is independent¹⁶ of whether it is on Cd^{11} , O , P , Al , etc.). This gives a good reason for the observation of similarly shaped curves for all the different systems studied within a particular distortion coordinate. What is perhaps surprising is that all these curves are superimposable if $r_i(\theta_{\text{dist}}) - r_i(\theta_{\text{undist}})$ is plotted against θ because the energy units of the interaction (the β 's and S 's) do vary from one system to another.

We have plotted in our curves values of $-\Delta_i$ against θ and compared them with the Δr_i vs. θ curves. Clearly the bond length is expected to increase as the bond stabilization energy decreases, but recall that we calculated this at geometries where all MX bond lengths are equal. Thus our method underestimates bond lengthening and overestimates bond shortenings since the relevant overlap integrals probably decrease with increasing MX distance. The discrepancies between the calculated and observed curves in Figure 6 and between Figures 7 and 8 are qualitatively of this sort. (For the plot of Figure 8 an almost superimposable fit to the data of Figure 7 is achieved if the reciprocal of the d orbital stabilization energy is plotted.)

We deliberately neglected to mention two facts in our discussion of main-group, five-coordinate species which have a general bearing on the application of perturbation methods. (i) The stabilization energies for the SPY geometry in Table I indicated that $r_{\text{axial}}/r_{\text{basal}} > 1$. In fact, for all systems studied²⁷ (main-group and d^0 species) $r_a/r_b < 1$. (ii) The stabilization energies also indicate that $r_{\text{ax}}/r_{\text{eq}} = 1$ for the TBP, but the axial bonds (for main-group and d^0 systems) are always longer than the equatorial bonds.^{27,30} We have rationalized both of these experimental observations previously¹⁴ by looking at the fourth power of the series expansion in the overlap integral (eq 3) of which eq 4 represents the leading term. There we assumed that $Ms-X\sigma$ and $Mp-X\sigma$ interactions were completely se-

parable in contrast to this present analysis. The result was that the stronger bonds are those that share the largest number of central-atom p orbitals with the smallest number of ligands, a concept which has been recognized for several years.

In this main-group, five-coordinate case there is perhaps competition between the "forces" of the present analysis (sp mixing) and the p -orbital sharing "forces". The bond lengths at the extreme ends of the Berry spectrum are clearly consistent with the dominance of the latter. However application of the p -orbital sharing method to the C_{3v} distortion of the tetrahedron leads to a strengthening of the axial and weakening of the basal bonds as θ increases by considering the quartic term of eq 3. (The quadratic terms with p orbitals alone are angle independent.) This is the reverse of the experimental observation, and here then sp mixing effects appear to be dominant. For the five-coordinate, transition-metal d^9 system, however, the observed geometry changes fitted very well the d -orbital-only model just by considering the angular variation in the quadratic term in eq 3.

In conclusion then, we are building¹⁴ a hierarchy via perturbation theory of structure-determining forces in molecules. If the quadratic term of eq 3 is angle dependent, then this may suffice to tell us what we need (e.g., the $d^{8,9}$ five-coordinate problem above). If this is angle independent as it is for most of the systems we have tackled here (and is also¹¹ for some unsaturated transition-metal systems, e.g., $Cr(CO)_4$), then the quartic powers of eq 3 (we have described elsewhere³¹ some of the applications of this particular approach) or the orbital mixing process needs to be considered. At present we are unable to say which will be larger in a given instance, although in some geometries (e.g., TBP MX_5) sp mixing is not allowed by symmetry.

Acknowledgment. I thank Drs. H.-B. Bürgi and P. Murray-Rust for several useful discussions and for making available work prior to publication.

References and Notes

- H.-B. Bürgi, *Inorg. Chem.*, **12**, 2321 (1973).
- H.-B. Bürgi, J. D. Dunitz, and E. Shefler, *J. Am. Chem. Soc.*, **95**, 5065 (1973).
- (a) P. Murray-Rust, H.-B. Bürgi, and J. D. Dunitz, *J. Am. Chem. Soc.*, **97**, 921 (1975). (b) For analogous structural correlations in germanates and silicates (especially minerals) see R. J. Hill, S. J. Louisnathan, and G. V. Gibbs, *Aust. J. Chem.*, **30**, 1673 (1977); J. A. Tossell and G. V. Gibbs, *Trans. Am. Geophys. Union*, **58**, 522 (1977), and references therein.
- P. Murray-Rust and J. Murray-Rust, *Acta Crystallogr., Sect. A*, **31**, S64 (1975).
- H.-B. Bürgi, *Angew. Chem., Int. Ed. Engl.*, **14**, 460 (1975).
- P. Murray-Rust, H.-B. Bürgi, and J. D. Dunitz, submitted for publication.
- P. Murray-Rust, private communication; J. L. Schlenker, D. T. Griffen, M. W. Phillips, and G. V. Gibbs, *Contrib. Mineral. Petrol.*, **65**, 347 (1978).
- L. Pauling, "The Nature of the Chemical Bond", 3rd ed., Cornell University Press, Ithaca, NY, 1963, p 246.
- (a) C. E. Schäffer and C. K. Jørgensen, *Mol. Phys.*, **9**, 401 (1965); (b) C. E. Schäffer, *Pure Appl. Chem.*, **24**, 361 (1970); M. Gerloch and R. C. Slade, "Ligand Field Parameters", Cambridge University Press, New York, 1973.
- J. K. Burdett, *Adv. Inorg. Chem. Radiochem.*, **21**, 113 (1978).
- J. K. Burdett, *Inorg. Chem.*, **14**, 375 (1975).
- J. K. Burdett, *Inorg. Chem.*, **14**, 931 (1975).
- J. K. Burdett, *Inorg. Chem.*, **16**, 3013 (1977).
- J. K. Burdett, *Struct. Bonding (Berlin)*, **31**, 67 (1976).
- E. M. Shustorovich, *Inorg. Chem.*, **17**, 2648 (1978).
- For an exhaustive list of overlap integrals between an orbital on a central atom (s, p, d, f) and a ligand orbital (σ, π, δ) as a function of geometry see W. Smith and D. W. Clack, *Rev. Roum. Chim.*, **20**, 1243 (1975).
- J. K. Burdett, R. C. Fay, and R. Hoffmann, *Inorg. Chem.*, **17**, 2553 (1978).
- A justification for this arises from a consideration of Badger's rule (force constant = $\partial^2 V / \partial r^2 = kr^{-3}$). The stabilization energy of the bond should then be inversely proportional to the bond length ($V \propto 1/r^3$). Thus $r_i \propto 1/[2\beta_p S_p^2 + (f(\theta))\beta_p S_p^2]$ and $\Delta r_i = -\Delta_i/[2\beta_p S_p^2 + (f(\theta))\beta_p S_p^2]$ so that the change in bond length is set by a combination of $Ms-X\sigma$ and $Mp-X\sigma$ forces. Whatever the exact dependence of stabilization energy and bond length, we expect bonds to shorten as the stabilization energy increases.
- W. H. Baur, *Acta Crystallogr., Sect. B*, **30**, 1195 (1974).
- M. Barrow, H.-B. Bürgi, D. K. Johnson, and L. M. Venanzi, *J. Am. Chem. Soc.*, **98**, 2356 (1976).

- (21) W. Clegg, *Acta Crystallogr., Sect. B*, **32**, 2712 (1976).
 (22) An alternative scheme which also leads to a rationalization of this behavior for these d^{10} systems is the ds (rather than sp) mixing process. See L. E. Orgel, *J. Chem. Soc.*, 4186 (1958).
 (23) Y. W. Yared, S. L. Miles, R. Bau, and C. A. Reed, *J. Am. Chem. Soc.*, **99**, 7076 (1977).
 (24) J. K. Burdett, *J. Chem. Soc., Faraday Trans. 2*, **70**, 1599 (1974).
 (25) M. Elian and R. Hoffmann, *Inorg. Chem.*, **14**, 1058 (1975).
 (26) In the case of these d^{10} transition-metal systems where the M_s orbital may be high in energy, we may no longer be able to neglect the interaction energy of M_p with the deepest lying a_1 orbital. In the present case, inclusion of this interaction tends to reduce the size of the effects we have described.
 (27) E. L. Muetterties and L. J. Guggenberger, *J. Am. Chem. Soc.*, **96**, 1748 (1974).
 (28) R. Hoffmann, *Acc. Chem. Res.*, **4**, 1 (1971).
 (29) This serves only to redistribute charge from one center to another within a single orbital. The reverse always occurs in the other occupied orbital involved in the mixing.
 (30) For the d^{10} systems $CdCl_3^{3-}$ and more strikingly $HgCl_3^{3-}$, the axial bond lengths are shorter than the equatorial. Shustorovich¹⁵ has rationalized this nicely on the basis of sd mixing (rather than the sp mixing we treat here) by use of his perturbation theory approach.¹⁵
 (31) T. A. Albright and J. K. Burdett, to be submitted for publication.
 (32) K. N. Raymond, P. W. R. Corfield, and J. A. Ibers, *Inorg. Chem.*, **7**, 1362 (1968).

Contribution from the Department of Chemistry,
 Cornell University, Ithaca, New York 14853

Perturbation Approach to the Substitution Effects in σ -Bonded Coordination Compounds

EVGENY SHUSTOROVICH

Received October 18, 1978

An analytical approach, in the framework of the perturbation theory of canonical LCAO MO's, to the effects of substitution of L by L' in various σ -bonded coordination compounds, EL_m (E is a transition metal M or main group element A, $m = 4-7$), has been developed. The compounds in question include the square EL_4 , octahedral EL_6 , trigonal EL_5 , and pentagonal EL_7 bipyramidal complexes. The difference in σ -orbital energies, $\delta\alpha' = \alpha(L') - \alpha(L)$, where $\delta\alpha' > 0$ (< 0) correspond to a better donor (acceptor) substituent L', was taken as a perturbation, and changes in overlap population of all the nonequivalent E-L bonds, $\delta N(E-L)/\delta\alpha'$, were obtained in terms of the ns , np , and $(n-1)d$ contributions. It was found that in all transition-metal complexes, ML_m , the s and d contributions to $\delta N(M-L_{tr})/\delta\alpha'$ ($tr = trans$) are always negative and bigger in absolute value than the p one which is always positive. The s and d contributions to $\delta N(M-L_{cis})/\delta\alpha'$ are always of opposite sign, typically the s one positive and the d one negative, so that $\delta N(M-L_{cis})$ will be smaller in absolute value than $\delta N(M-L_{tr})$ and may be of any sign. The effects of substitution in the main-group element complexes AL_m , for which the hypervalent structure (with only ns and np valence orbitals) has been assumed, strongly depend on the oxidation state of the central atom. If A is of the highest oxidation state, under axial substitution the s and p contributions to $\delta N(A-L_{tr})/\delta\alpha'$ are typically of opposite sign, the s one positive and the p one negative. The relative values of these contributions and the resulting sign of $\delta N(A-L_{tr})/\delta\alpha'$ can depend not only on the nature of A and L but also on the type of polyhedra, AL_m . At the same time, for all AL_m polyhedra, the only contribution to $\delta N(A-L_{cis})/\delta\alpha'$, the s one, is always negative. If A is not of the highest oxidation state, both the s and p contributions to $\delta N(A-L_{tr})/\delta\alpha'$ are always negative, but $\delta N(A-L_{cis})/\delta\alpha' = 0$. Under equatorial substitution, specifically for EL_5 and EL_7 complexes, the regularities for $\delta N(E-L_{cis})/\delta\alpha'$ remain the same as those under axial substitution, but the regularities for $\delta N(E-L_{eq})/\delta\alpha'$ prove to be even more varied than those for $\delta N(E-L_{tr})/\delta\alpha'$. In particular, in pentagonal-bipyramidal EL_7 complexes, the values of $\delta N(E-L_{\theta})/\delta\alpha'$ for two nonequivalent equatorial ligands L_{θ} (forming valence angles $\theta = 2\pi/5$ and $4\pi/5$ with L') may be of opposite sign. The role of π -bonding effects is also briefly discussed. The results obtained explain the nature and peculiarities of the fundamental substitution effects, particularly the $trans$ and cis influence, and permit a number of predictions for scarcely studied compounds, specifically $AL_{m-k}L'_k$, to be made.

Introduction

All the possible polyhedra EL_m can be divided into two groups depending on the existence, or lack, of the geometrical equivalence of the $m-1$ ligands L with respect to the substituent L' in the $EL_{m-1}L'$ complex. The first group where all ligands L are equivalent include linear ELL' , planar-trigonal EL_2L' and tetrahedral EL_3L' compounds. The second group where not all the ligands L are equivalent include square EL_3L' , octahedral EL_5L' , trigonal-bipyramidal (TB) EL_4L' and pentagonal-bipyramidal (PB) EL_6L' complexes. The effects of substitution in complexes of the first group are the same for each L, and we have already considered this problem in another paper.¹ The purpose of the present work is to consider the effects of substitution in complexes of the second group.² The different geometrical positions in the polyhedra in question are shown in Figure 1. As earlier,¹⁻³ we choose the overlap population $N(E-L)$ as a criterion of the E-L bond strength. Further, we adopt the difference in diagonal matrix elements (ligand σ -orbital energies)

$$\langle \sigma_L | H | \sigma_{L'} \rangle - \langle \sigma_L | H | \sigma_L \rangle = \delta\alpha' \quad (1)$$

as a perturbation, so that, to first order, all changes in $N(E-L)$

for a given ligand L will be (the closed shell case)

$$\frac{\delta N(E-L)}{\delta\alpha'} = \sum_{\chi} \sum_i \sum_j \frac{c_{i\chi} c_{jL'} (c_{i\chi} c_{jL} + c_{j\chi} c_{iL}) S_{\chi L}}{\epsilon_i - \epsilon_j} \quad (2)$$

Here the LCAO MO coefficients c and energies ϵ are designated by the indices where χ refers to AO's of the central atom E ($\chi = s, p, d$) and i and j refer to the occupied and vacant canonical MO's, respectively, $S_{\chi L} = \langle \chi | \sigma_L \rangle$. Finally, for every bonding canonical MO

$$\psi = c_E \chi_E + c_L \theta_L \quad (3)$$

we shall use as its antibonding counterpart

$$\psi^* = c_L \chi_E - c_E \theta_L \quad (4)$$

where χ_E is an AO of the central atom E and θ_L is a symmetry-adapted group orbital formed from the σ_L orbitals, $c_E^2 + c_L^2 = 1$. All the interrelations between the coefficients c_E and c_L , the energies $\epsilon(\psi)$ and $\epsilon(\psi^*)$, and other necessary formulas may be found in ref 1 and 3.

Results and Discussion

Square Complexes $EL_4 D_{4h}$, $16e d^8 ML_4$. Let us begin with transition-metal complexes $d^8 ML_4$ where we shall consider